Available online at www.sciencedirect.com
SCIENCE DIRECT®
PERGAMON
International Journal of Heat and Mass Transfer 46 (2003) 2353–2361
International Journal of HEAT and MASS TRANSFER
www.elsevier.com/locate/ijhmt

Boiling heat transfer and dryout phenomenon of CO_2 in a horizontal smooth tube

Rin Yun [a], Yongchan Kim [a,*], Min Soo Kim [b], Youngdon Choi [a]

[a] Department of Mechanical Engineering, Korea University, Anam-dong, Sungbuk-ku, Seoul 136-701, South Korea
[b] Department of Mechanical and Aerospace Engineering, Seoul National University, Seoul 151-744, South Korea

Received 17 May 2002; received in revised form 25 November 2002

Abstract

Evaporation heat transfer characteristics of carbon dioxide (CO_2) in a horizontal tube are experimentally investigated. The test tube has an inner diameter of 6.0 mm, a wall thickness of 1.0 mm, and a length of 1.4 m. Experiments are conducted at saturation temperatures of 5 and 10 °C, mass fluxes from 170 to 320 kg/m^2 s and heat fluxes from 10 to 20 kW/m^2. Partial dryout of CO_2 occurs at a lower quality as compared to the conventional refrigerants due to a higher bubble growth within the liquid film and a higher liquid droplet entrainment, resulting a rapid decrease of heat transfer coefficients. The effects of mass flux, heat flux, and evaporating temperature are explained by introducing unique properties of CO_2, flow patterns, and dryout phenomenon. In addition, the heat transfer coefficient of CO_2 is on average 47% higher than that of R134a at the same operating conditions. The Gungor and Winterton correlation shows poor prediction of the boiling heat transfer coefficient of CO_2 at low mass flux, while it yields good estimation at high mass flux.

Keywords: CO_2; Evaporation heat transfer; Boiling; Dryout; Horizontal smooth tube

1. Introduction

Due to environmental concerns and corresponding regulations, hydrofluorocarbon (HFC) refrigerant mixtures such as R410A have been considered as the primary replacements for R22, by far the most commonly used refrigerant for air-conditioning applications. In recent years, carbon dioxide (CO_2) has been reintroduced as a possible R22 replacement because CO_2 naturally exists in the atmosphere and has a lower global warming potential (GWP) than HFCs. The potential applications of CO_2 include heat pump water heaters, mobile air conditioners and heat pumps, and military environmental control units.

Recent research related with CO_2 heat exchangers has been focused on the acquisition of heat transfer data and the development of a heat transfer correlation during the evaporation and gas cooling processes. Bredesen et al. [1] measured the boiling heat transfer coefficients of CO_2 in a 7.0 mm inner diameter tube by varying heat flux, mass flux, and saturation temperature. They observed that dryout occurred only at an evaporation temperature of 5 °C. They also found that the heat transfer coefficient significantly increased with a rise of heat flux in the low-quality region, but the effects of mass flux were relatively small as compared to those of heat flux. Zhao et al. [2] measured the evaporation heat transfer coefficients of CO_2 by varying mass fluxes from 160 to 320 kg/m^2 s, heat fluxes from 10 to 20 kW/m^2, and at an evaporating temperature of 10 °C in a 6.0 mm inner diameter tube. They showed that the influence of heat flux on the heat transfer coefficient was relatively significant at all qualities, while it was relatively small at high mass flux. Hwang et al. [3] proposed a boiling heat transfer correlation for CO_2 by modifying the Bennett–Chen correlation. Their correlation was consistent with Bredesen et al.'s [1] data within a deviation of 14%.

* Corresponding author. Tel.: +82-2-3290-3366; fax: +82-2-921-5439.
E-mail address: yongckim@korea.ac.kr (Y. Kim).

0017-9310/03/$ - see front matter © 2003 Elsevier Science Ltd. All rights reserved.
doi:10.1016/S0017-9310(02)00540-9

Nomenclature

D	tube diameter (m)
F, Fr	modified Froude number
G	mass flux (kg/m^2 s)
g	acceleration due to gravity (m/s^2)
h	heat transfer coefficient (W/m^2 K)
h_{le}	heat transfer coefficient for entire liquid flow (W/m^2 K)
h_{lv}	latent heat of vaporization (J/kg)
k	thermal conductivity (W/m K)
L_H	heated length (m)
$\dot{m}_{lfc}, \bar{\dot{m}}_{lfc}$	critical film flow rate at the onset of entrainment (kg/m^2 s), averaged
q''	heat flux (W/m^2)
T	temperature (°C, K)
U	velocity in x-direction (m/s)
$w_e, \bar{w}_e$	entrained mass flux (kg/m^2 s), averaged
x	vapor quality

Greek symbols

α	angle between the pipe axis and the horizontal, positive for downward flow
ρ	density (kg/m^3)
γ	dimensionless number
μ	dynamic viscosity (N s/m^2)
δ	liquid film thickness (m)
δ_L	liquid level
τ_i	interfacial shear stress (N/m^2)
σ	surface tension (N/m)
ξ	diameter ratio, dimensionless

Subscripts

crit	critical
g	vapor
l	liquid
o	outside
s	superficial
sat	saturation
ss	stainless steel
sup	suppression
w	inner tube wall

Due to a high operating pressure of CO_2, recently microchannel and small diameter tubes had received significant interest as a possible replacement of the conventional fin-tube geometry. Pettersen et al. [4] and Zhao et al. [5] investigated the evaporation heat transfer of CO_2 in microchannels. They found that prior to dryout quality, the effects of heat flux on the heat transfer coefficient were relatively larger than those of mass flux. The variation of heat transfer coefficients with respect to quality was very small. In addition, the dryout quality decreased with an increase of mass flux. These are consistent well with the test results of Tran et al. [6] and Peter and Keith [7] in small diameter tubes.

Even though many evaporation heat transfer data of CO_2 are available in the open literature, only few studies have addressed the fundamental boiling phenomena of CO_2 and the effects of dryout and its prediction method. The objective of this study is to explain the fundamental heat transfer characteristics of CO_2 in a horizontal tube by using unique properties of CO_2, flow patterns and dryout phenomenon. In addition, the heat transfer coefficients of CO_2 are compared with those of R134a.

2. Experimental setup and test conditions

A schematic of the experimental setup is shown in Fig. 1. The test loop consists of a liquid pump, a mass flow meter, a preheater, a test section, and a condenser. The inlet quality of the test section is adjusted by an electric power input to the preheater. The refrigerant having a high quality at the exit of the test section is completely condensed and subcooled by the condenser. The magnetic gear pump circulates the refrigerant passing through the test section. The control tank that is kept inside of a constant temperature bath is connected to the suction side of the pump to allow easy regulation of refrigerant charge. Varying charge amount of CO_2 in the system controls operating pressure in the system.

The test tube is made of stainless steel with a heated length of 1400 mm, and outside and inside diameters of 8.0 and 6.0 mm, respectively. Applying a direct current heating method provides heat flux to the test section. Since the electrical resistance of the tube is approximately 0.058 Ω, a high-current transformer with a maximum current and voltage of 120 A and 20 V, respectively, is used to supply heat flux. Thermocouples are placed at the top, the bottom, and the sides at each location, which is equally located along the test section with an interval of 200 mm. The junctions are electrically insulated from the tube using a very thin Teflon tape. The test section is insulated using a rubber with a thermal conductivity of 0.04 W/m K to minimize heat loss to the ambient. The heat loss is estimated by comparing electric heat input with actual heat transfer to the refrigerant. The heat loss is within 5% of the electric heat input at an average refrigerant temperature of 10 °C, and it is taken into account in the experiments and

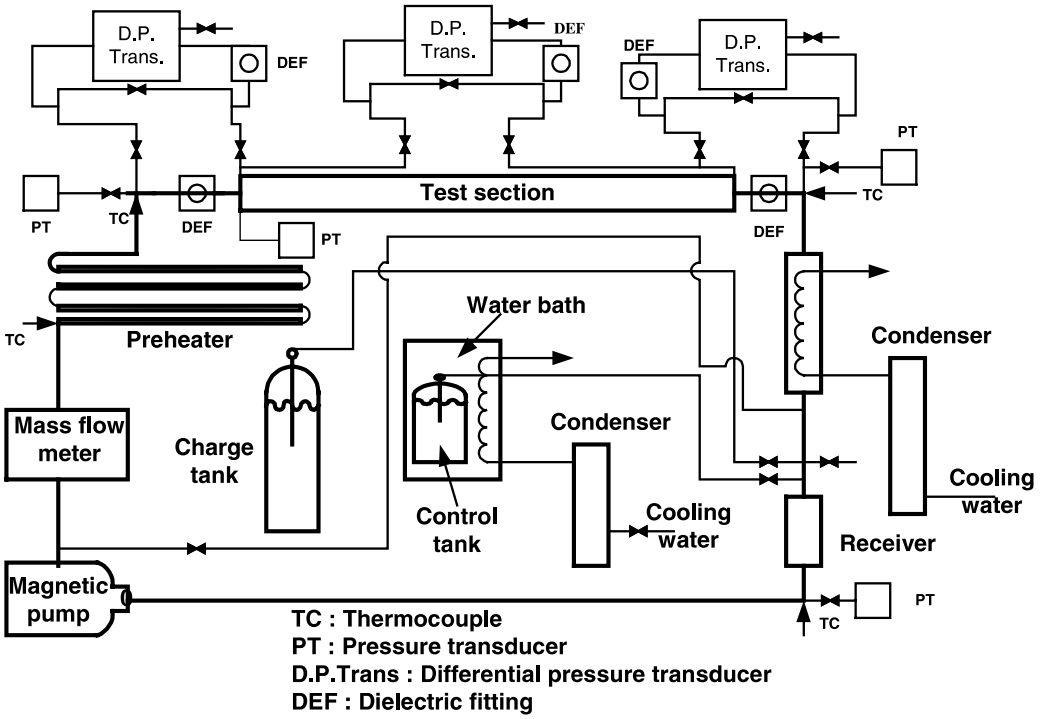

Fig. 1. Schematic of the test setup.

analysis of the test data. Using dielectric fittings before and after the test section prevents an electric leakage to the other parts of the test setup.

The refrigerant flow rate is measured using a Coriolis effect flow meter with an uncertainty of ±0.2% of reading. The pressures of the refrigerant at the inlet and outlet of the test section are monitored using a pressure transducer with an uncertainty of ±2.1 kPa, while the pressure drop across the test section is measured using a differential pressure transducer. Wall temperatures of the test section and refrigerant temperatures are measured by T-type thermocouples with a calibrated accuracy of ±0.1 °C. The temperature differences among the thermocouples during single-phase runs are less than ±0.2 °C.

Evaporation heat transfer coefficients are measured with a variation of mass flux, heat flux, and saturation temperature. The mass flux is varied at 170, 240, and 320 kg/m^2 s, while the heat flux is altered at 10, 15, and 20 kW/m^2 with evaporating temperatures of 5 and 10 °C.

3. Data reduction

The local heat transfer coefficient, h, inside a smooth tube is determined from the measured heat flux, q'', the refrigerant temperature, T_r, and the calculated inside wall temperature, T_w.

$$h = q''/(T_w - T_r) \tag{1}$$

The inside wall temperature, T_w, is calculated from the measured outside wall temperatures, $T_{w,o}$, using both the equation of steady state radial heat conduction through the tube and heat generation within the tube wall [8].

$$T_w = T_{w,o} + \left(\frac{q''}{4\pi k_{ss} L_H}\right)\left[\frac{\xi(1-\ln\xi)-1}{1-\xi}\right] \tag{2}$$

where $\xi = (D_O/D)^2$.

The corresponding bulk temperatures of CO_2 at each axial position are determined by using an interpolation method with an assumption of a linear temperature gradient in the bulk fluid over the heated length. The estimated uncertainty of heat transfer coefficient is ±8.0% at average conditions with a heat flux of 20 kW/m^2 [9].

4. Results and discussion

Fig. 2 shows the heat transfer coefficients and expected flow patterns of CO_2 with respect to mass flux and heat flux. Generally, the heat transfer coefficients of CO_2 decrease with an increase of quality. However, the conventional refrigerants such as R134a, R410A, and R22 show an increment of the evaporation heat transfer coefficient with a rise of quality. The drop in heat

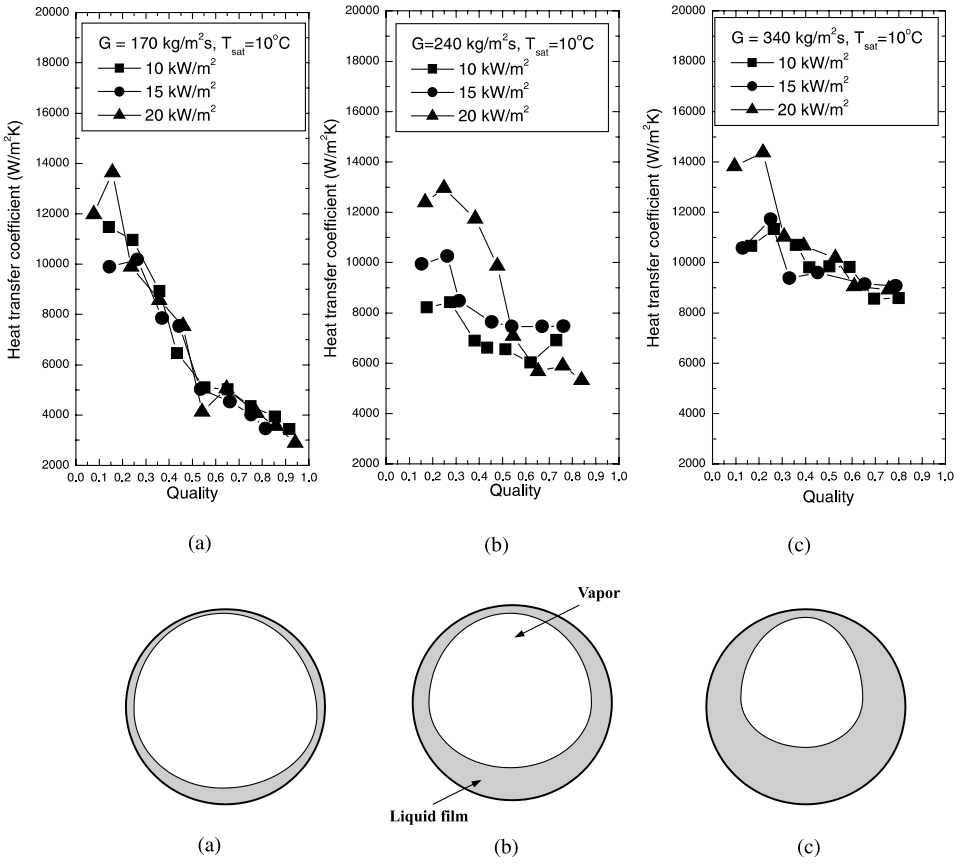

Fig. 2. Effects of flow patterns on heat transfer coefficients.

transfer coefficient with quality in Fig. 2 is due to both partial dryout of liquid film at a lower quality and dominance of nucleate boiling at low qualities. The partial dryout of CO_2 that is represented by a rapid drop of heat transfer coefficients with respect to quality occurs at a lower quality as compared to that for the conventional refrigerants. Thermophysical properties of CO_2 such as a lower surface tension and a lower density ratio of liquid to vapor cause the dominance of nucleate boiling at low qualities.

Generally, CO_2 includes much more liquid in the early stage of the evaporation process with a lower vapor velocity because the density ratio of ρ_l/ρ_g is relatively low. Therefore, the ratio of liquid level, δ_L, to tube diameter, D, may be greater than 0.5 during the evaporation process of CO_2 at low qualities, which leads to an intermittent flow [10]. As the evaporation proceeds with a rise of quality, the flow pattern can be changed from intermittent to annular flow with a gradual decrease of δ_L.

Kefer et al. [11] explained the effect of tube orientation on a boiling crisis in terms of F as given in Eq. (3) [10]. For $F \geqslant 10$, the tube orientation shows hardly any influence on the boiling crisis, while for $F < 7$, the evaporation process is in unstable, asymmetric annular flow, which yields significant influence of tube orientation on the boiling crisis. As shown in Table 1, since the value of F in this study, which slightly increases with a rise of mass flux, is less than 3, unstable asymmetric annular flow may occur dominantly. Due to liquid droplet entrainment from the liquid film, the flow pattern in this case exists in unstable annular mist flow. Inoue and Lee [12] showed that the existence of unstable annular mist flow increased the possibility of the occurrence of critical heat flux (CHF). Generally, liquid entrainment flux is significantly higher at the bottom of the tube than at the top [13]. As shown in Fig. 2, since the liquid film becomes thicker with an increase in mass flux, the slope of the heat transfer coefficient vs. quality changes significantly with respect to mass flux.

$$F = \sqrt{\frac{\rho_g}{(\rho_l - \rho_g)}} \frac{U_{s,g}}{\sqrt{Dg\cos\alpha}} \tag{3}$$

Bubble growth in the liquid film and liquid droplet entrainment cause the occurrence of dryout patches

Table 1
Effects of tube orientation on a boiling crisis in terms of F

	Mass flux (kg/m^2 s)					
	170		240		340	
Evaporating temperature (°C)	5	10	5	10	5	10
F [10]	1.17	1.12	1.66	1.58	2.34	2.24

[12,14]. A lower surface tension of CO_2 accelerates bubble growth in the liquid film. Since CO_2 has much lower surface tension than the conventional refrigerants, more active nucleation sites at a specified heat flux exist. This would also increase the probability of liquid droplet entrainment resulted from bursting of bubbles [15]. Furthermore, the suppression of the nucleate boiling will be delayed due to a lower vapor velocity. When the suppression quality, x_{sup}, at which the nucleation is suppressed, is determined by using Eqs. (4) and (5) [16], the x_{sup} of CO_2 is twice as much as that for the conventional refrigerants. Therefore, the formation of dryout patches during the evaporation of CO_2 becomes easier due to a higher bubble growth rate and a higher suppression quality as compared to the conventional refrigerants.

$$x_{sup} = \frac{\gamma}{1+\gamma} \tag{4}$$

$$\gamma = \left(\frac{\rho_g}{\rho_l}\right)^{0.56}\left(\frac{\mu_l}{\mu_g}\right)^{0.11}\left(\frac{q'' k_l h_{lv} \rho_g}{98\sigma T_{sat} h_{le}^2}\right)^{1.11} \tag{5}$$

A higher liquid entrainment of CO_2 in an annular flow would also accelerate the formation of dryout patches. The mass flux of entrained liquid droplet for CO_2 during the convective evaporation process is higher than that for the conventional refrigerants due to a relatively thick liquid film. As shown in Eq. (6) suggested by Stevanovic and Studovic [17], the entrained mass flux, w_e, is proportional to the exponent of liquid film thickness, δ. The liquid film thickness of CO_2, which is estimated by using an annular flow model [18], is approximately twice as large as that for R22.

$$w_e = 1.1 \times 10^4 \times \delta^{2.25} \times \rho_l \tag{6}$$

The critical film flow rate of CO_2 that determines the onset of liquid droplet entrainment is smaller than that of other conventional refrigerants. In Eq. (7) correlated by Hewitt and Govan [19], $\dot{m}_{lfc}$ depicts the critical film flow rate. As the $\dot{m}_{lfc}$ decreases, the possibility of early dryout during the evaporation process increases.

$$\dot{m}_{lfc} = \mu_l \times \exp\left(5.8504 + 0.4249 \times \frac{\mu_g}{\mu_l}\sqrt{\frac{\rho_l}{\rho_g}}\right) \tag{7}$$

Fig. 3 shows the effects of heat flux on the heat transfer coefficient at a given mass flux. As the heat flux increases, the heat transfer coefficient is significantly

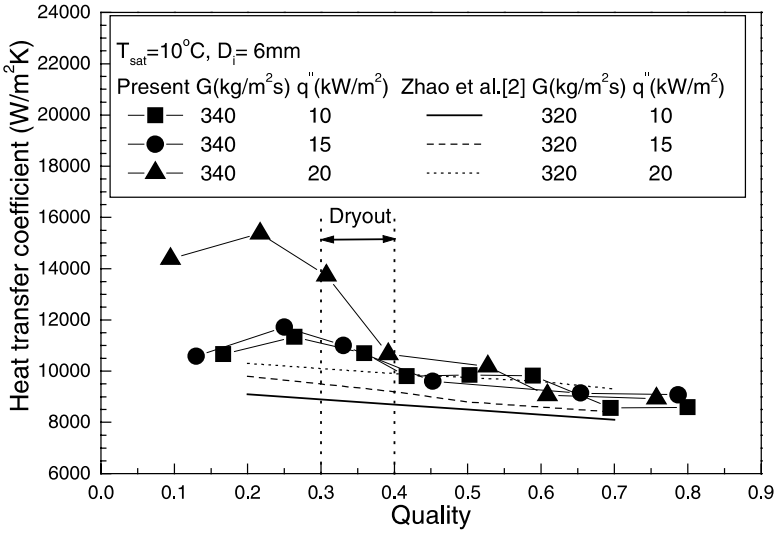

Fig. 3. Effects of heat flux.

improved at low qualities due to an increase of active nucleation site. However, after the partial dryout occurs at the quality of 0.3–0.4, the effects of heat flux decrease. Fig. 3 includes the data of Zhao et al. [2] that were measured using the water heating method in a 6.0 mm ID tube at the similar test conditions as this study. Zhao et al. [2] showed that the heat transfer coefficient increased with a rise of heat flux at all qualities, which results in some difference from the present data at high qualities. The heat transfer coefficients observed by Zhao et al. [2] linearly decreased with an increase of quality, but a distinct dryout quality was not observed. It is noticeable that the partial dryout at all heat fluxes occurs at the qualities from 0.3 to 0.4, because the dryout quality is determined by the liquid film thickness that is strongly dependent on mass flux.

Fig. 4 shows the variation of heat transfer coefficients with respect to mass flux. For qualities from 0.2 to 0.5, the heat transfer coefficient is independent of mass flux because the nucleate boiling is dominant in this region. Hihara and Tanaka [20] and Pettersen et al. [4] also observed this trend in their experiments. For qualities above 0.5, the heat transfer coefficient increases with a rise of mass flux due to an enhancement of convective evaporation. As the mass flux increases at high qualities, dry patches are rewetted and the dryout quality becomes higher.

Fig. 5 shows the effects of evaporating temperature on heat transfer coefficients based on the data from this study and Cho et al. [21]. Although the heat flux of this study is higher than that of Cho et al. [21], the trends of heat transfer coefficients can be compared each other due to the similarity on the effects of evaporating temperature. In the present data, the heat transfer coefficient at low quality increases with a rise of evaporating temperature, while for high quality it decreases with an increase of evaporating temperature. These trends were also observed in the test results of Pettersen et al. [4]. Besides, as shown in Fig. 5(b), Cho et al. [21] showed the same trends as the evaporating temperature increases from −10 to 5 °C, but the heat transfer coefficients increases at all qualities as the evaporating temperature increases from −25 to −10 °C.

As the evaporating temperature increases at low qualities, not only the nucleate boiling becomes more active but also the liquid film thickness becomes thinner, reducing its thermal resistance and thereby enhancing heat transfer coefficient. However, as the evaporating temperature increases at high qualities, the heat transfer coefficients are more rapidly reduced with respect to quality due to the formation of dryout patches in annular mist flow. Table 2 represents the results of Eqs. (4)–(7) evaluated by using the annular flow model [18] with a variation of evaporating temperature. As a result, it can be concluded that the formation of dryout patches becomes easier with an increase in evaporating temperature.

Fig. 6 shows the comparison of the heat transfer coefficients for CO_2 with those for R134a. For qualities less than 0.5, the heat transfer coefficient of CO_2 is on average 56% higher than that of R134a, while for all qualities tested, it is higher by 47% on average. Besides, the effect of heat flux on heat transfer coefficients of CO_2 is much more pronounced than that of R134a. For low qualities, the nucleate boiling of CO_2 is more active than that of R134a due to its lower vapor velocity and higher suppression quality of nucleate boiling. For medium and high qualities, the liquid film of CO_2 is relatively thin, which is alternately dried and rewetted. On the contrary, R134a shows a stable annular flow pattern and a lower

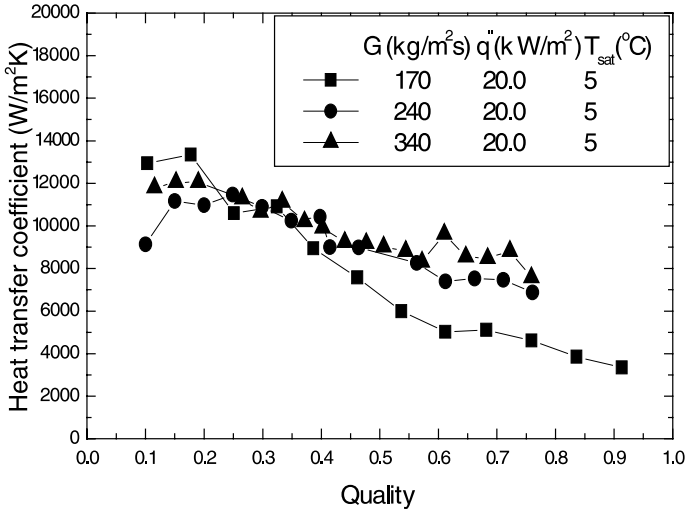

Fig. 4. Effects of mass flux.

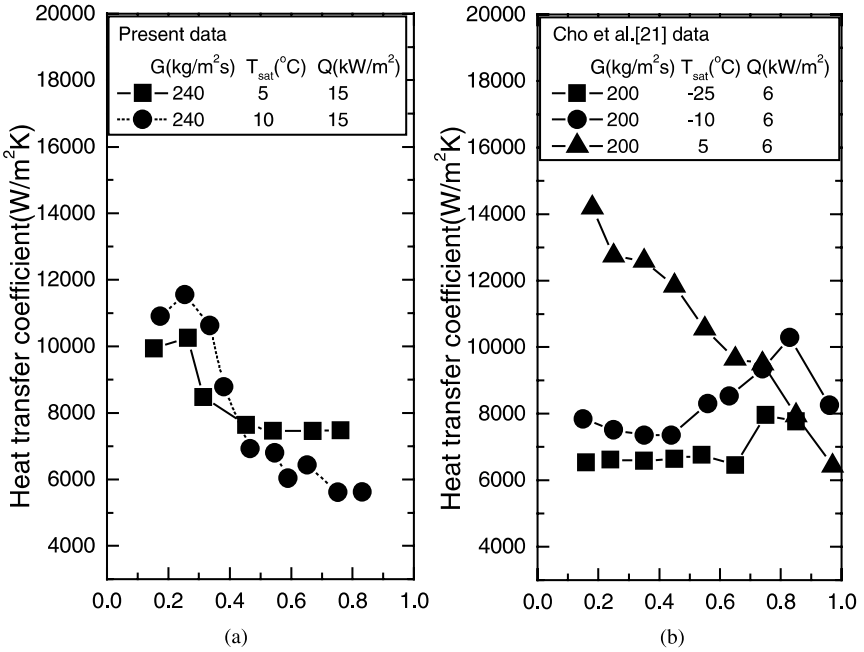

Fig. 5. Effects of evaporating temperature.

Table 2
Results of Eqs. (4)–(7) at $q'' = 15$ kW/m^2, $G = 300$ kg/m^2 s, and $D = 6.0$ mm

Temperature (°C)	σ (N/m)	x_{sup}	$\bar{w}_e$, Eq. (6) (kg/m^2 s)	$\tau_i\delta/\sigma$[a]	$\bar{\dot{m}}_{lfc}$ (kg/m^2 s)
0	4.55×10^{-3}	0.98	0.28	1.93	7.30
10 °C	2.77×10^{-3}	0.99	0.32	3.03	6.07

[a] $w_e \propto (\tau_i\delta/\sigma)^n$ $(n > 0)$ [22].

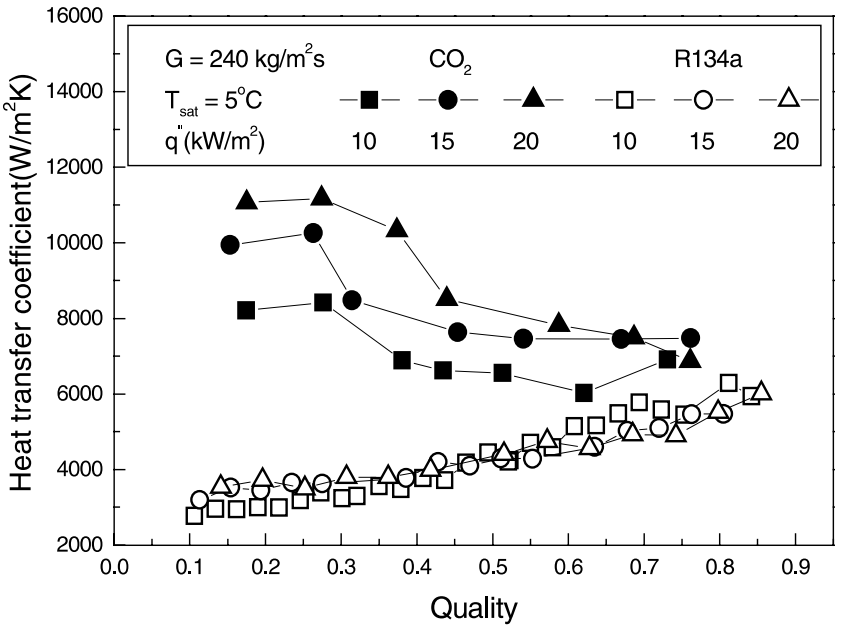

Fig. 6. Comparisons of heat transfer coefficients for CO_2 with those for R134a.

liquid droplet entrainment as compared to CO_2. The liquid film for R134a can be retained much longer on the tube wall. Therefore, the heat transfer coefficient of CO_2 decreases while that of R134a increases with a rise of quality.

Table 3 shows the deviations between the Gungor and Winterton correlation [23] and the present data. The Gungor and Winterton correlation [23] assumed that the convective boiling becomes dominant with an increase of quality due to the suppression of the nucleate boiling. In addition, their correlation was developed for stable annular flow. However, CO_2 at low mass flux represents relatively wide nucleate boiling dominant region. Besides, CO_2 at low mass flux exists alternately in intermittent flow, unstable annular flow and dryout conditions with an increase of quality. Therefore, the Gungor and Winterton correlation [23] shows large deviations at a mass flux of 170 kg/m^2 s. However, as the mass flux increases, not only the suppression quality becomes smaller but also stable annular flow becomes a dominant flow pattern. Therefore, for high mass flux, the Gungor and Winterton correlation yields good agreement with the data of this study, [1,2,21].

The dryout qualities (or critical qualities) in a horizontal and an inclined tube predicted by the Ahmad method [24] and Kefer et al. [11], respectively, are given in Table 3. The term of $x_{crit,upper}$ indicates a critical quality including the effects of tube orientation in an inclined tube. Generally, the critical qualities decrease with a rise of mass flux. Comparing Fig. 2 with x_{crit} in Table 3 shows some deviations between the measured and the predicted values. However, the Ahmad method well estimates the existence of dryout for the data in the literature: this study, [1,2,21].

5. Conclusions

Boiling heat transfer characteristics of CO_2 in a horizontal tube are investigated as a function of mass flux, heat flux, and evaporating temperature. Generally, the heat transfer coefficient of CO_2 decreases with an increase of quality due to both a lower dryout quality and dominance of nucleate boiling as compared to the conventional refrigerants. The dryout of CO_2 is accelerated by bubble growth in the liquid film and liquid droplet entrainment in unstable annular or annular mist flow because of a lower surface tension, a higher suppression quality, and a lower critical film flow rate. As the heat flux increases, the heat transfer coefficients are significantly enhanced at low qualities, while the effects of heat flux decrease after the dryout occurs. The effects of mass flux on the heat transfer coefficient are relatively small at low and moderate qualities, but the mass flux plays an important role in determining dryout quality. The heat transfer coefficients at low qualities increase

Table 3
Comparison of the Gungor and Winterton correlation [23] with the test data, and dryout quality

Mass flux (kg/m^2 s)																				
170						240						340								
Evaporation temperature (°C)	5	5	5	10	10	10	5	5	5	10	10	10	5	5	5	10	10	10		
Heat flux (kW/m^2)	10	15	20	10	15	20	10	15	20	10	15	20	10	15	20	5	15	20		
Mean deviation (%)	45.2	38.1	55.1	46.5	46.1	67.0	18.4	12.4	16.8	29.6	31.0	34.6	12.0	9.7	10.5	18.3	10.2	13.9		
Average deviation (%)	−36.9	−26.2	−43.4	−28.8	−41.0	−59.9	−13.3	−5.1	−7.3	−21.5	−22.8	−20.6	10.0	7.0	3.0	18.0	2.9	10.99		
x_{crit} [24]	0.99	0.94	0.91	0.88	0.84	0.81	0.88	0.84	0.81	0.79	0.75	0.72	0.79	0.75	0.72	0.70	0.66	0.64		
$x_{crit,upper}$[a] [11]	0.78	0.72	0.67	0.62	0.56	0.52	0.73	0.68	0.64	0.59	0.54	0.50	0.68	0.63	0.60	0.56	0.52	0.48		

[a] $x_{crit,upper} = x_{crit} - 16.0/(2 + Fr)^2$, $Fr = x_{crit}G/\sqrt{gD(\rho_l - \rho_g)\cos\alpha\rho_g}$.

with a rise of evaporating temperature because of a thin liquid film on the wall, while the heat transfer coefficients at high qualities are rapidly reduced with respect to quality due to an easy formation of dryout patches. In addition, the Gungor and Winterton correlation shows large deviations from the present data at low mass flux, but it yields good agreement with the data at high mass flux.

Acknowledgements

This work was jointly supported by the Korea Science and Engineering Foundation (grant no. 1999-1-304-006-3), the Korea University, and the Micro Thermal System Research Center.

References

[1] A.M. Bredesen, A. Hafner, J. Pettersen, P. Neksa, K. Afleckt, Heat transfer and pressure drop for in-tube evaporation of CO_2, in: Proceedings of the International Conference on Heat Transfer Issues in Natural Refrigerants, College Park, MD, 1997, pp. 1–15.

[2] Y. Zhao, M.M. Ohadi, S.V. Dessiatoun, M. Molki, J. Darabi, Forced convection boiling heat transfer of CO_2 in horizontal tubes, in: AJTE99-6249, Proceedings of the Fifth ASME/JSME Joint Thermal Engineering Conference, San Diego, CA, 1999.

[3] Y. Hwang, B. Kim, R. Radermacher, Boiling heat transfer correlation for carbon dioxide, in: Proceedings of the International Conference on Heat Transfer Issues in Natural Refrigerant, College Park, MD, 1997, pp. 44–57.

[4] J. Pettersen, R. Rieberer, S.T. Munkejord, Heat transfer and pressure drop characteristics of evaporating carbon dioxide in microchannel tubes, in: Fourth IIR-Gustav Lorentzen Conference on Natural Working Fluids, Purdue University, 2000, pp. 107–114.

[5] Y. Zhao, M Molki, M.M. Ohadi, Heat transfer and pressure drop of CO_2 flow boiling in microchannels, in: Proceedings of the International Mechanical Engineering Congress and Exposition, Orlando, FL, 2000.

[6] T.N. Tran, M.W. Wambsganss, D.M. France, Boiling heat transfer with three fluids in small circular and rectangular channels, Argonne National Laboratory, ANL-95/9, 1995.

[7] A.K. Peter, C. Keith, Correlations for the prediction of boiling heat transfer in small-diameter channels, Appl. Thermal Eng. 17 (1997) 705–715.

[8] M.W. Wambsganss, D.M. France, J.A. Jendrzejczyk, T.N. Tran, Boiling heat transfer in a horizontal small-diameter tube, J. Heat Transfer 115 (1993) 963–972.

[9] R.J. Moffat, Using uncertainty analysis in the planning of an experiment, J. Fluids Eng. 107 (1985) 173–178.

[10] Y. Taitel, A.E. Dukler, A model for predicting flow regime transitions in horizontal and near horizontal gas–liquid flow, AIChE J. 22 (1) (1976) 47–55.

[11] V. Kefer, W. Köhler, W. Kastner, Critical heat flux and post-CHF heat transfer in horizontal and inclined evaporator tubes, Int. J. Multiphase Flow 15 (3) (1989) 385–392.

[12] A. Inoue, S. Lee, Influence of two-phase flow characteristic on critical heat flux in low pressure, in: International Conference on Nuclear Engineering, vol. 1, ASME, 1996, pp. 657–667.

[13] D. Butterworth, D.J. Pulling, A visual study of mechanisms in horizontal, annular, air–water flow, AERE-M2556, 1972.

[14] J. Pettersen, Flow vaporization of CO_2 in microchannel tubes, Part 1: Experimental method and two-phase flow, in: Fifth IIR-Gustav Lorentzen Conference on Natural Working Fluids, Guangzhou, China, 2002, pp. 76–83.

[15] T. Fujita, T. Ueda, Heat transfer to falling liquid films and film breakdown II (saturated liquid films with nucleate boiling), Int. J. Heat Mass Transfer 21 (1978) 109–118.

[16] T. Sato, H. Matsumura, On the conditions of incipient subcooled-boiling with forced convection, Bull. JSME 7 (26) (1964) 392–398.

[17] V. Stevanovic, M. Studovic, A simple model for vertical annular and horizontal stratified two-phase flows with liquid entrainment and phase transitions: one-dimensional steady state conditions, Nucl. Eng. Design 154 (1995) 357–379.

[18] V.P. Carey, Liquid–Vapor Phase-Change Phenomena, Taylor & Francis, 1992, pp. 439–448.

[19] G.F. Hewitt, A.H. Govan, Phenomenological modeling of non-equilibrium flows with phase change, Int. J. Heat Mass Transfer 33 (2) (1990) 229–242.

[20] E. Hihara, S. Tanaka, Boiling heat transfer of carbon dioxide in horizontal tubes, in: Fourth IIR-Gustav Lorentzen Conference on Natural Working Fluids, Purdue University, 2000, pp. 279–284.

[21] E.S. Cho, S.H. Yoon, M.S. Kim, A study on the characteristics of evaporative heat transfer for carbon dioxide in a horizontal tube, in: Proceedings of the KSME Spring Annual Meeting, 2000, pp. 104–107.

[22] P. Hutchinson, P.B. Whalley, A possible characterization of entrainment in annular flow, Chem. Eng. Sci. 28 (1973) 974–975.

[23] K.E. Gungor, R.H.S. Winterton, A general correlation for flow boiling in tubes and annuli, Int. J. Heat Mass Transfer 29 (1986) 351–358.

[24] S.Y. Ahmad, Fluid to fluid modeling of critical heat flux: a compensated distortion model, Int. J. Heat Mass Transfer 16 (1973) 641–662.